organics

MDPI

Article

Unveiling the Origin of the Selectivity and the Molecular Mechanism in the [3+2] Cycloaddition Reaction of N-aryl-C-carbamoylnitrone with N-arylitaconimide

Abdelmalek Khorief Nacereddine [1,*] and Fouad Chafaa [1,2]

[1] Laboratory of Physical Chemistry and Biology of Materials, Department of Physics and Chemistry, Higher Normal School of Technological Education-Skikda, Azzaba, Skikda 21300, Algeria
[2] Faculty of Natural, Life Sciences University of Batna 2, Batna 05078, Algeria
* Correspondence: a.khorief@enset-skikda.dz

Abstract: The [3+2] cycloaddition reaction of N-aryl-C-carbamoylnitrone (nitrone **1**) with N-arylitaconimide (ethylene **2**) was computationally studied using the B3LYP/6-31G(d) level of theory. An analysis of the different energetic profiles and the transition states' optimized structures clearly indicated that this 32CA occurred through a non-polar, asynchronous, one-step mechanism, favoring the formation of the *ortho–endo* cycloadduct, as observed experimentally. The analysis of the reactivity indices derived from the conceptual DFT explains well the low polarity of this 32CA reaction. Parr functions and a dual reactivity descriptors analysis correctly explained the regioselectivity *ortho* of this 32CA reaction. Solvent effects did not modify the obtained selectivity but it increased the activation energies and decreased the exothermic character of this 32CA reaction. A thermodynamic parameters analysis indicated that this 32CA wascharacterized by an *ortho* regioselectivity and endostereoselectivity and exothermic and exergonic characters.

Keywords: mechanism; regioselectivity; stereoselectivity; cycloaddition; DFT calculations

Citation: Khorief Nacereddine, A.; Chafaa, F. Unveiling the Origin of the Selectivity and the Molecular Mechanism in the [3+2] Cycloaddition Reaction of N-aryl-C-carbamoylnitrone with N-arylitaconimide. *Organics* **2022**, *3*, 281–292. https://doi.org/10.3390/org3030021

Academic Editors: Wim Dehaen, Michal Szostak and Huaping Xu

Received: 7 May 2022
Accepted: 17 August 2022
Published: 2 September 2022

1. Introduction

Heterocyclic compounds are important structures as they have a great importance in biological and pharmaceutical fields [1]. They are considered promising targets and central unit structures in the drug discovery process [2]. The most important pharmaceutical properties of heterocyclic compounds are antidepressant [3], antimicrobial [4], antibacterial [5] and anticancer [6]. The large spectrum of the applications of these compounds made scientists interested in the synthesis of this type of molecule with increased biological activities. Heterocycles are important scaffolds that are used extensively as replacement structures of functional groups in order to modulate the polarity of the drug and, therefore, increase its bioavailability [7].

Isoxazolidines are important heterocycles which contain five atoms, with N and O atoms in an adjacent position. Due to their different biological activities, the synthesis of these types of molecules has been the essential axis of many research groups. Additionally, they have been used as synthetic intermediates, namely for β-amino alcohol preparation. In addition, these compounds have been used for anticonvulsant, antibiotic and antitubercular activities [8,9]. One of the most important methods for the preparation of this kind of molecule is the [3+2] cycloaddition (32CA) reaction between nitrones and alkenes [10]. The 32CA reaction is an important and efficient synthetic method that is used extensively for the synthesis of tremendous five-membered nitrogen-, oxygen- and sulfur-containing heterocyclic compounds [11]. Many natural and synthetic biologically active molecules contain spiroheterocycles [12]. These compounds are endowed by many unique properties [13]. Thereby, these compounds have many applications in many fields [14,15] and thus they are

largely used as constructive molecules in order to synthesize biologically active, relevant molecules [16,17].

The challenge today in organic synthesis is how to prepare pure compounds with a high yield using a simple and efficient method. The main goal of theoretical chemists in the prediction or the interpretation of certain chemical procedure results is understanding and improving the properties of these procedures and their products. Understanding the factors controlling the selectivity of organic reactions may help with controlling the peri-, chemo-, regio-, stereo-and diastereoselectivity of the preparation of pure, biologically actives molecules [18].

Nitrones are three atomic components (TACs) [19] which may react with various types of unsaturated skeletons to produce heterocyclic scaffolds [20]. The reactivity behaviors of these important TAC structures depends on the substituent and also on the reactive partner. Thus, it can react as an electrophile [21–23], especially when it possesses an electron-withdrawing group at the carbon atom of the nitrone system, as well as where the dipolarophilepossesses an electron-realizing group, which enhances its nucleophilicity. On the other hand, in major cases, the nitrone is classified as a nucleophile [24,25], in which it reacts with a large amount of electrophilic dipolarophiles.

An interesting case of a 32CA reaction involving N-aryl-C-carbamoylnitrone (nitrone **1**) and N-arylitaconimide (ethylene **2**) was described recently by Teterina et al. [26] In this 32CA reaction, a mixture of stereoisomeric [3+2] cycloadductswasformed, in which one cycloadduct was obtained with a major quantity (10/1) (Scheme 1).

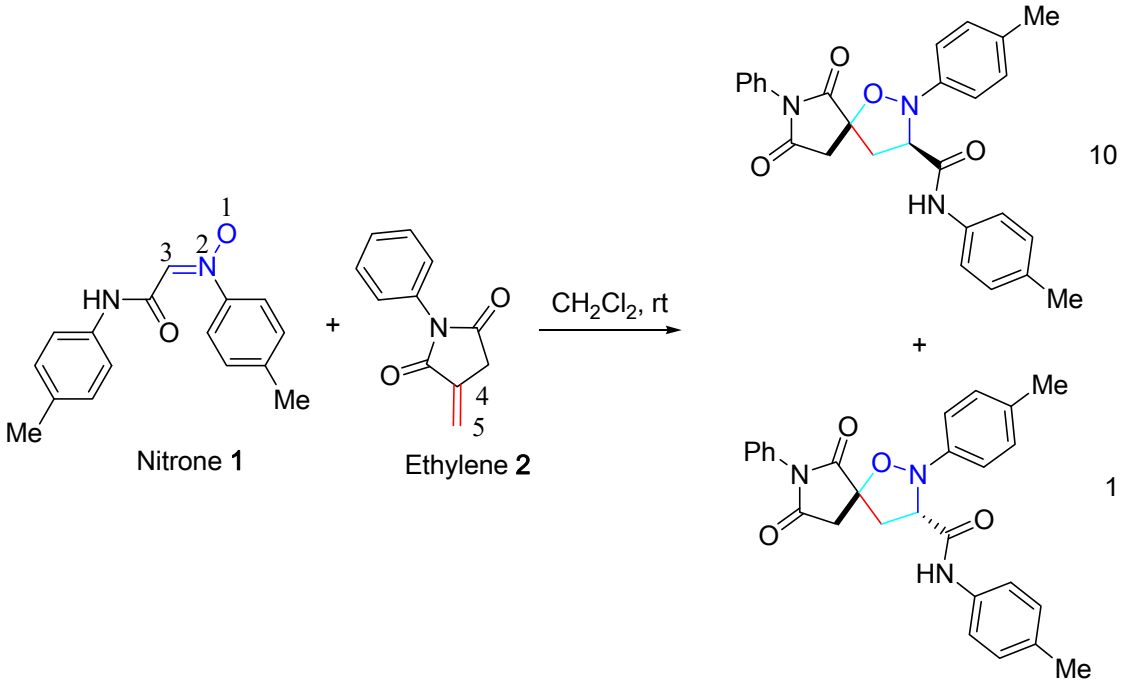

Scheme 1. 32CA reaction between N-aryl-C-carbamoylnitrone **1** and N-arylitaconimide **2**.

Our axis of research focuses on explaining the origin of the regio- and stereoselectivities, as well as the molecular mechanism nature, of organic reactions, namely cycloaddition reactions [27–31]. The main goal of this work is to understand the origin of regio- and stereoselectivities as well as the molecular mechanism of the32CA reaction performed by Teterina et al. [26] through a MEDT [32] study.

2. Computational Methods

In order to perform this MEDT study, we used the following programs and methods:

- The Gaussian 09 [33] was used for the optimization of all the stationery points, namely, the reagents, transition states and cycloadducts.

- The B3LYP/6-31G(d) was the used for the DFT method for all the calculations [34–36].
- The frequency calculations were used to confirm that the optimized stationery points were TSs or minimums. The structure of the TSs were used to confirm that the mechanism was one step or stepwise by performing intrinsic reaction coordinate (IRC) calculations [37], in which the obtained curve indicates that the TS structure is connected to the two minimums, in the forward direction to the cycloadduct and in the reverse direction to the separated reagents.
- The solvent effects of dichloromethane were investigated using the polarizable continuum model (PCM) [36–38] within the self-consistent reaction field (SCRF) [39–41] through single-point calculations on the optimized gas phase structures.
- The values of thermochemistry properties such as Gibbs free energies, enthalpies and entropies were calculated using standard statistical thermodynamics at 298.15 K and 1 atm through the optimized gas phase structures [42].
- The electrophilicity index (ω) [43], which is a measure of the molecule's ability to accept electrons, is given by the relation $\omega = (\mu^2/2\eta)$.
- The electronic chemical potential (μ) and the chemical hardness (η) were calculated directly from the energies of the frontier molecular orbitals ε_{HOMO} and ε_{LUMO}, respectively, by the following relations: $\mu = (\varepsilon_{HOMO} + \varepsilon_{LUMO})/2$ and $\eta = \varepsilon_{LUMO} - \varepsilon_{HOMO}$ [44].
- The nucleophilic index [45], (*N*), which is a measure of the molecular power of the donating electrons, is given by the relation $N = \varepsilon_{HOMO(Nu)} - \varepsilon_{HOMO(TCE)}$, in which TCE is tetracyanoethylene, which is taken as the reference due to its low HOMO energy.
- The Parr functions [46], namely, the electrophilic index (P_K^+) and nucleophilic one (P_K^-), which allowed us to characterize the most electrophilic and nucleophilic atoms in a molecule, were obtained by an analysis of the Mulliken atomic spin density of the radical anion and the radical cation, respectively, of the studied molecule.
- The dual reactivity descriptors were used in order to determine, atthe same time, the nucleophilic and the electrophilic atomic region in the studied molecule. These descriptors were obtained from the difference between nucleophilic and electrophilic Fukui functions [47] as follow:

$$\Delta f(r) \approx f^+(r) - f^-(r) = \rho_{N+1}(r) + \rho_{N-1}(r) - 2\rho_N(r)$$

  where ρ_{N+1} ®®$_{(r)}$ an®$_{N-1}$(r) are the electronic densities at point *r* for a system with (N + 1), (N) and (N − 1) electrons, respectively.

- The Wiberg bond indices were used to analyze the synchronicity of the mechanism [48].
- The global electron density transfer (GEDT) [49] was calculated with the natural atomic charges (*q*). These lasts were obtained by a natural population analysis (NPA) computation [50].

3. Results and Discussion

This part is divided into three sections: first, we begin our study by analyzing the global reactivity descriptors of the separated reactants and the local reactivity indices to determine the regioselectivity and the reactivity of the reagents associated with this 32CA reaction. In the second section, we perform an analysis on the geometries and polar character of this 32CA reaction. In the last section, an analysis of the energetic profiles of all the reactive paths through the gas phase, in solution and finally with consideration of all the experimental conditions, such as temperature (25 °C), solvent nature (dichloromethane) and pressure (1 atmosphere), is conducted.

3.1. Analysis of Reactivity

Several previous studies on cycloaddition reactions showed that CDFT reactivity descriptors are important tools to predict the reactivity of organic reagents in their ground

state [51–54]. Thus, the conceptual DFT global reactivity indices [55] were calculated using the mentioned equations (see above) and are gathered in Table 1.

Table 1. CDFT global reactivity indices of nitrone **1** and ethylene **2** (in eV).

Reactant	HOMO	LUMO	μ	η	ω	*N*
Nitrone **1**	−5.74	−2.05	−3.89	3.68	2.06	3.39
Ethylene **2**	−6.39	−1.80	−4.09	4.58	1.83	2.74

From Table 1, the values of the global reactivity μ of both nitrone **1** and ethylene **2** clearly indicate that nitrone **1** had the highest value, indicating the flux direction of the GEDT from nitrone **1** towards ethylene **2**. Thus, nitrone **1** will react as a nucleophile, while ethylene **2** as an electrophile. Otherwise, by comparing the electrophilicity indices of both reagents, we can notice that nitrone **1** (ω = 2.06 eV) is more electrophilic than ethylene **2** (ω = 1.83 eV). This behavior is in contradiction with what was obtained using electronic chemical potential behavior. On the other hand, the nucleophilicity indices analysis indicated that nitrone **1** (N = 3.39 eV) is a more nucleophilic reagent than ethylene **2** (N = 2.74 eV), in agreement with the electronic chemical potential analysis and in contradiction with the electrophilicity indices analysis. In addition, we can notice that all the reactivity indices of both reactants are close, indicating that the 32CA reaction between them will occur with a low polar character. This fact may be due to the presence of electron-withdrawing groups in both reagents, namely, the amide function.

3.1.1. Analysis of Regioselectivity Using Parr Functions

The local Parr function indices together with their atomic spin density (ASD), 3D maps of the radical anions ofnitrone **1** and ethylene **2** and the radical cations ofnitrone **1** and ethylene **2** are illustrated in Figure 1.

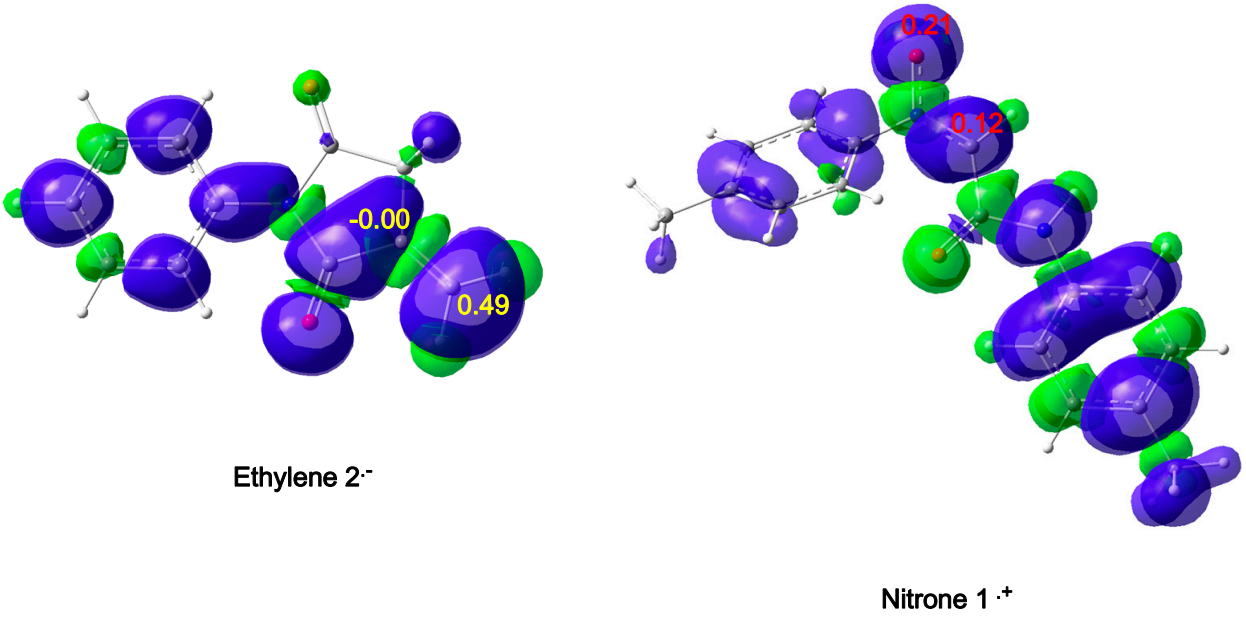

Figure 1. *Cont.*

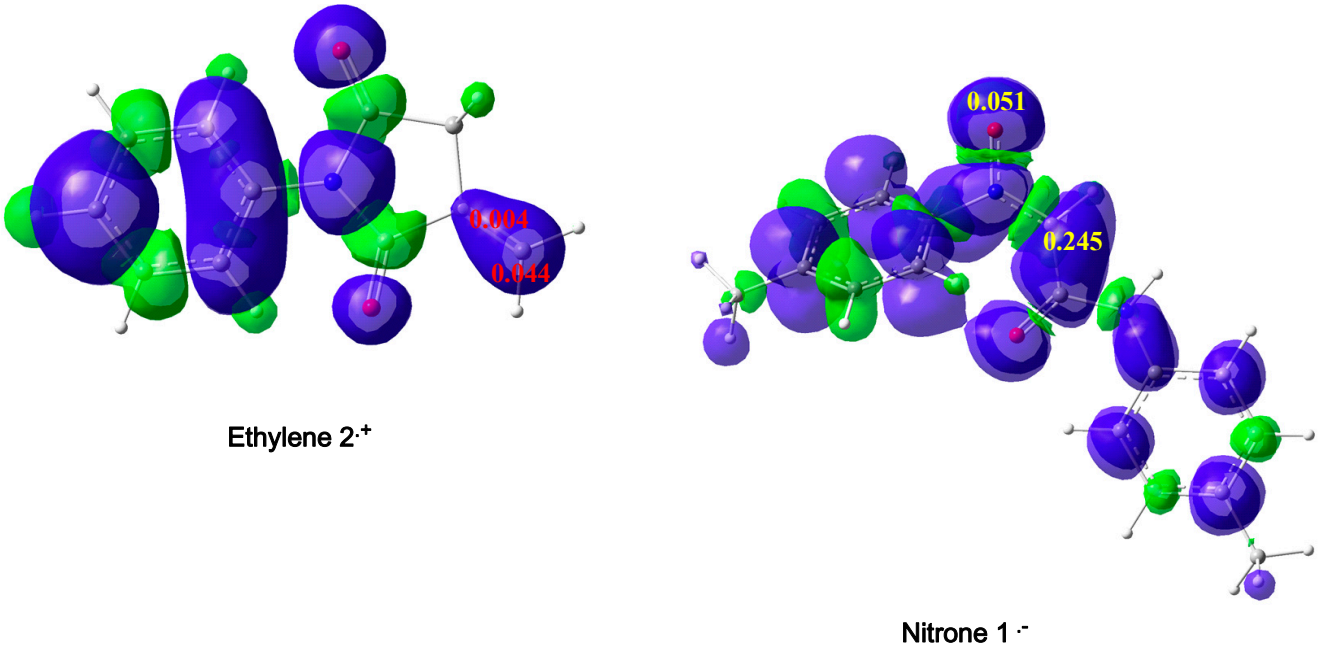

Figure 1. 3D maps of the ASD representation (isovalue = 0.006) of cations of nitrone 1^+ and ethylene 2^+ and anions of ethylene 2^- and nitrone 1^- together with the nucleophilic $P^-{}_K$ indices (in red) and electrophilic $P^+{}_K$ indices (in yellow), as well as the Parr function values of their reactive atoms.

First, we began our analysis by the proposition that nitrone **1** is a nucleophile and ethylene **2** is an electrophile. Thus, an analysis of the electrophilic P_K^+ Parr function of ethylene **2** indicated that the carbon atom C5 (for atom numbering, see Scheme 1) is the most electrophilic center, with $P_{C5}^+ = 0.49$. For nitrone **1**, the most electrophilic center is located on the O1 oxygen atom with $P_{O1}^+ = 0.21$. Consequently, the most nucleophilic center (O_1) of the nucleophile (nitrone **1**) will interact with the most electrophilic center (C_5) of the electrophile (ethylene **2**), leading to the formation of a *meta* regioisomer, in contradiction with the experimental data.

For the nucleophilic P_K^- Parr function indices, we can notice that the highest index in ethylene **2** is located at carbon atom C5 ($P_{C5}^- = 0.044$) while, for the electrophilic P_K^+ Parr function indices of nitrone **1**, the highest value is located at carbon atom C3 ($P_{C3}^- = 0.245$). Consequently, the favorable interaction between the nucleophilic center and the electrophilic center is that between (C_5) of ethylene **2** with C_3 of nitrone **1**, generating the *ortho* regioisomer cycloadducts, in agreement with the experimental data. Therefore, nitrone **1** is the electrophilic reagent and ethylene **2** is the nucleophilic one.

Using Dual Descriptors

Figure 2 shows the dual reactivity descriptors tri-dimensional (3D) maps of nitrone **1** and ethylene **2**. Note that the turquoise lobes indicate the nucleophilic regions, while the purple lobes indicate the electrophilic regions. Thus, for the nitrone **1** reagent, an analysis of the dual descriptors corresponding to the reactive region O1=N2=C3 of nitrone **1** shows that O1 and C3 has a nucleophilic character while C3 has an electrophilic character. On the other hand, for ethylene 2, the C4 and C5 reactive atoms have an electrophilic character in which the C4 carbon atom is slightly more electrophilic than the C5 one. These behaviors indicate that the most plausible interaction will occur between the O1 reactive center of nitrone **1** and the C4 atom of ethylene **2**, allowing the formation of the *ortho* regioisomer cycloadducts, in great accordance with the experimental outcomes, energy profiles (see later) and Parr function analyses.

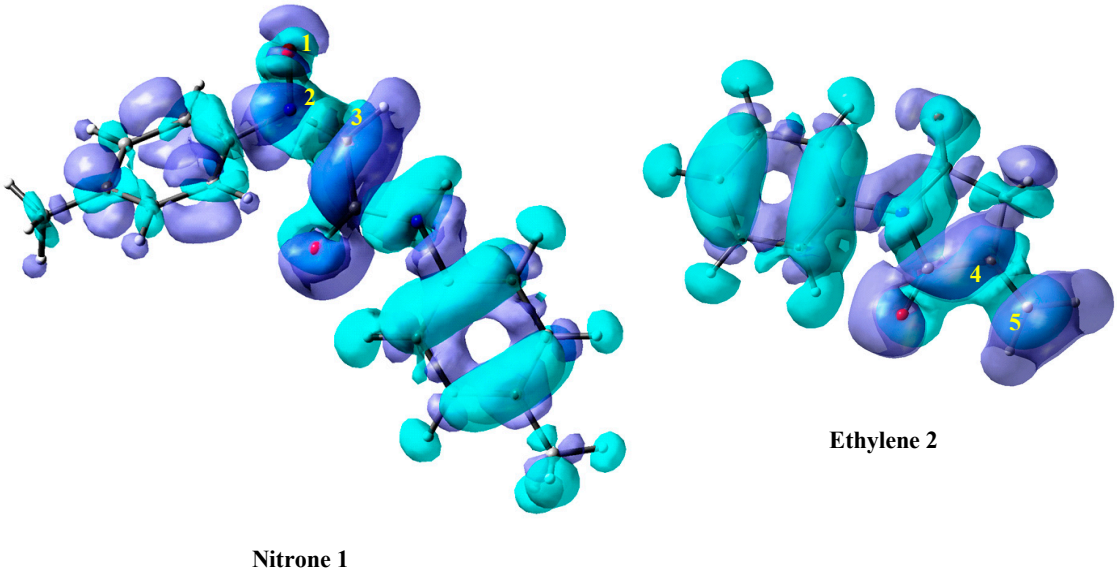

Figure 2. Maps of $\Delta f(r)$ dual descriptors for nitrone **1** and ethylene **2** with isovalue = 0.006.

3.2. Geometries of TSs and Reaction Polarity Analysis

The optimized structures of the transition states associated with the 32CA reaction of nitrone **2** with ethylene **1** together with the lengths of the new bonds and their Wiberg bond indices are given in Figure 3.

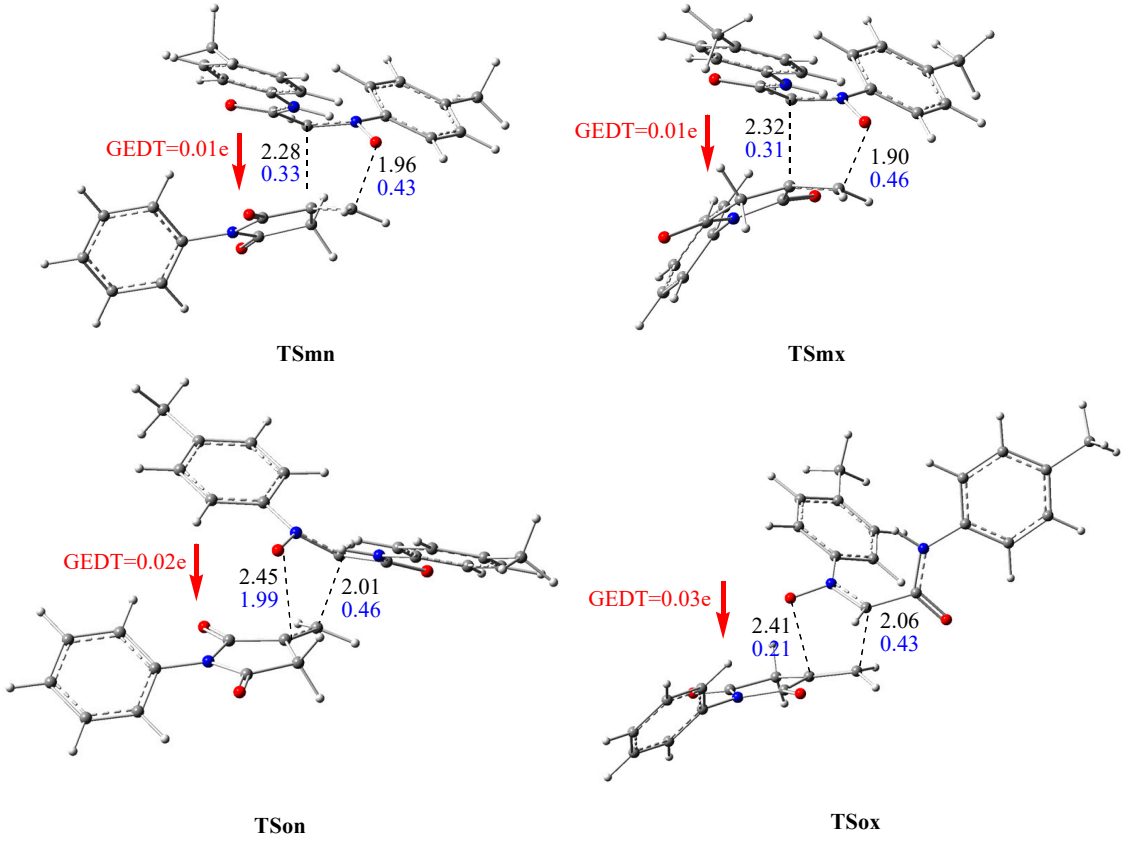

Figure 3. Optimized structures of the TSs of the 32CA reaction of nitrone **1** with ethylene **2** together with the lengths of the new bonds, the values of GEDT and the Wiberg bond indices (in blue).

From Figure 3, we can notice that the lengths of the new bonds O−C and C−C are 1.96 and 2.28 Å for the **TSmn** and 1.90 and 2.32 Å for the **TSmx**. In addition, in **TSox**, the

lengths of the O−C and C−C new bonds are 2.41 and 2.06 Å and in **TSon** the length of these bonds are 2.45 and 2.01 Å. Note that the C−C single bond formation occurs in a distance between 2.0–1.9 Å while the C−O one is between 1.8 and 1.7Å [19]. Thus, these values indicate an asynchronous mechanism for the *ortho* paths, in which the C−C new bond formation is more advanced than that of the C−O one. For the non-favored pathways, these geometrical parameters account for a synchronous mechanism.

An analysis using the Wiberg bond indices [48] was performed to confirm the nature of this mechanism through the NBO method [50].

The values of the BO associated with the C–O and C–C new bonds are 0.43 and 0.33 for **TSmn**, 0.46 and 0.31 for **TSmx**, 0.19 and 0.46 for **TSon** and 0.21 and 0.43 for **TSox**. We can notice at the *ortho* pathways that the C–C bond formation is more advanced than that of the C–C one.In contrast, for the *meta* paths, the mechanism is slightly synchronous.

The analysis of the GEDT values allows us to determine the polar character of this 32CA reaction. Indeed, several previous studies [56–58] established that the polar reactions are more feasible and precede faster with low activation energies [59]. Thus, for the studied 32CA reaction of nitrone **1** with ethylene **2**, the computed GEDT values were calculated at the ethylene **2** fragment, in which the negative values are an indicator for the way the flux of the GEDT comes from nitrone **1** towards ethylene **2**.

The values of the GEDT are 0.01e for **TSmn** and **TSmx**, 0.02e for **TSon** and 0.03e for **TSmx**. The very low values of the GEDT point out the non-polar character of this 32CA reaction, justifying well the similitude of the electronic properties as obtained previously in the CDFT reactivity indices analysis [60].

3.3. Energy Profiles Analysis

3.3.1. Gas Phase Electronic Energy Analysis

In general, in the cycloaddition reactions, when the structure of the reagents is asymmetric, we can have four reactive competitive pathways. Thus, the present 32CA reaction is the case, therefore, that we used to study two regioisomeric channels, the *ortho* and *meta*, and two stereoisomeric approaches, the *endo* and *exo*. Thereby, the four transition states are **TSmn**, **TSmx**, **TSon** and **TSox** and are associated with the corresponding cycloadducts **CAmn**, **CAmx**, **CAon** and **CAox**, respectively (See Scheme 2). The computed total and relative energies in the gas phase and in the dichloromethane solution of the stationery points involved in the present 32CA reaction are given in Table 2.

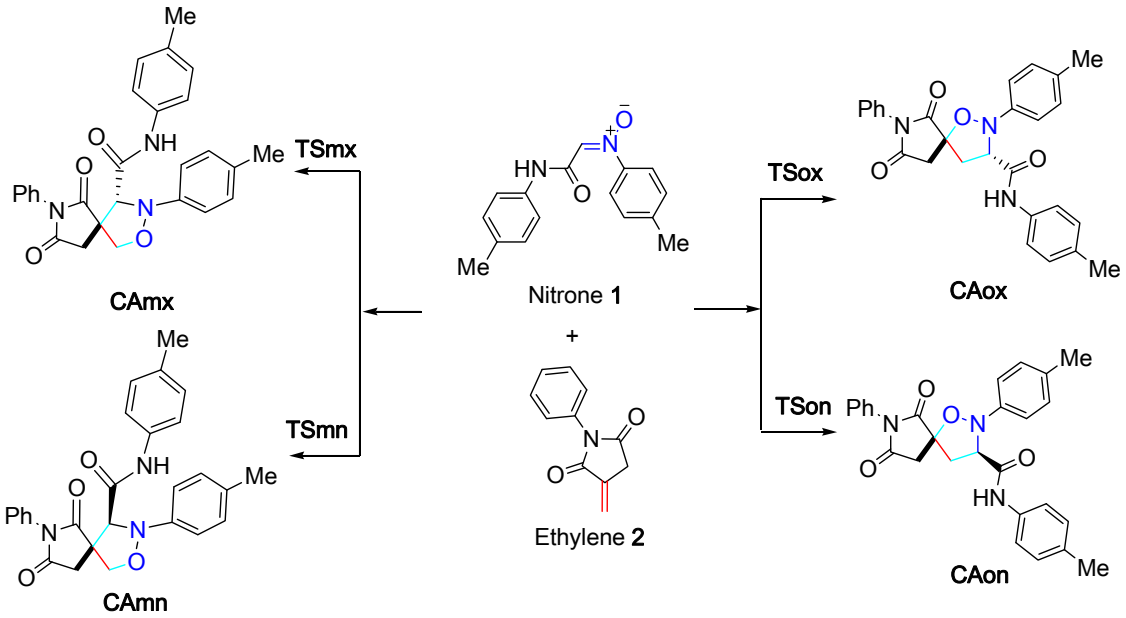

Scheme 2. The four reactive pathways of the 32CA reaction of nitrone **1** with ethylene **2**.

Table 2. Values of total and relative energy in gas phase and in dichloromethane solution of stationery points of the32CA reaction between nitrone **1** and ethylene **2**.

System	E (a.u)	ΔE (kcal/mol)	E (a.u)	ΔE (kcal/mol)
	Gas Phase		Dichloromethane	
Alkene	−629.81087		−629.823074	
Nitrone	−879.26189		−879.27378	
TSmn	−1509.06612	4.17	−1509.08303	8.68
TSmx	−1509.06713	3.54	−1509.08269	8.89
TSon	−1509.07438	−1.02	−1509.08977	4.45
TSox	−1509.05882	8.75	−1509.07558	13.36
CAmn	−1509.11571	−26.95	−1509.13108	−21.47
CAmx	−1509.11574	−26.97	−1509.13074	−21.26
CAon	−1509.12384	−32.05	−1509.13821	−25.95
CAox	−1509.11167	−24.41	−1509.12653	−18.62

From Table 2 and by an analysis of the gas phase energies, we clearly see that the *ortho–endo* approach has the lowest activation energy (E_a = −1.02 kcal/mol) and has a negative sign, which accounts for the corresponding cycloadduct being the kinetically favored cycloadduct, in which its formation is spontaneous ($E_a < 0$). Additionally, we can see that all the reactive paths are irreversible since the relative energies of the corresponding cycloadducts are negative ($\Delta E_{Cas} < 0$). Therefore, all the cycloadducts are stable compounds, indicating that the studied 32CA reaction is under a kinetic control, mainly leading to the formation of the cycloadduct **CAon**, in accordance with the experimental observations.

3.3.2. Solvent Effects

To shed light onto the solvation effects, we performed an analysis on the energy profiles, taking into account the nature of the solvent (dichloromethane) in our calculations. From Table 2 and by a comparison between the relative energy values in the gas phase and in the solution phase of the stationary points, namely, the transition states and cycloadducts, the remarkable change is an increase in the activation energies by values between 4 and 5 kcal mol^{-1}. In addition, there are decreases in the relative energies of the cycloadducts, which account for a decrease in the exothermic character of this 32CA reaction. The increase in the activation energies and the decrease in the exothermic character are mainly due to the better solvation of nitrone **1** and ethylene **2** than the corresponding TSs and CAs [61]. Therefore, the solvent does not make any changes on the selectivity observed in the gas phase study of this 32CA reaction.

3.3.3. Thermochemistry Analysis

Because this 32CA reaction occurred in the liquid phase and demanded certain experimental conditions, to study the effects of the experimental conditions of this 32CA reaction, we performed supplementary calculations on enthalpy, entropy and free energy, which were calculated by taking into account the temperature, pressure and nature of the solvent. The values of the total and relative thermochemistry parameters are given in Table 3.

From the values of the thermochemistry parameters, we can notice that the *ortho–exo* reactive pathway is always the more favored one. In addition, the exothermic character of this 32CA is not modified, since all the cycloadducts have negative values of relative enthalpy. On the other hand, the high values of the activation free energies that are increased by 11.10, 12.59, 12.85 and 13.99 when compared to the activation enthalpies for **Tson**, **Tsox**, **TSmn** and **TSmx**, respectively, are due to the consideration of the entropic contribution in the calculations. The negative sign of the relative free energies of the cycloadducts indicates that this 32CA reaction has an exergonic character. Consequently, the inclusion of the temperature, pressure and solvent nature in the calculations indicate that this 32CA is *ortho* regioselective under kinetic control and has exothermic and exergonic characters.

Table 3. Values of total and relative thermodynamic properties for the stationery points associated with the 32CA reaction of nitrone **1** with ethylene **2**.

System	H	ΔH	S	ΔS	G	ΔG
Alkene	−629.636002		102.186		−629.68453	
Nitrone	−878.976215		144.081		−879.044638	
TSon	−1508.600621	7.28	209.023	106.837	−1508.699885	18.38
Tsox	−1508.560719	32.31	204.023	101.837	−1508.657608	44.90
TSmn	−1508.568092	27.69	203.132	100.946	−1508.664558	40.54
TSmx	−1508.555116	35.83	199.318	97.132	−1508.649771	49.82
Caon	−1508.645213	−20.70	209.115	106.929	−1508.744521	−9.63
Caox	−1508.644865	−20.49	209.978	107.792	−1508.744583	−9.67
Camn	−1508.652843	−25.49	211.35	109.164	−1508.753212	−15.09
Camx	−1508.64097	−18.04	210.757	108.571	−1508.741057	−7.46

4. Conclusions

In this research work, we were able to carry out a computational study of regio- and stereoselectivities as well as on the molecular mechanism associated with the 32CA reaction of nitrone **1** with ethylene **2** within a B3LYP/6-31G(d) level of theory.

I. The CDFT global reactivity indices explain the low polar character of this 32CA reaction, which is related to the close electronic parameters of the reagents.
II. An analysis on reactivity and selectivity using the local indices obtained from the Parr functions explain well the experimentally *ortho* regioselectivity and indicates that nitrone **1** is an electrophile while ethylene **2** is a nucleophile.
III. The analysis of regioselectivity using dual reactivity indices allows us to explain well the observed *ortho* regioselectivity.
IV. The analysis of the molecular mechanism of this 32CA reaction using the GEDT and Wiberg indices indicated that it is a non-polar, one-step, asynchronous mechanism for the favored *ortho* pathways and synchronous for the *meta* ones.
V. The energy profile gas phase analysis showed that the studied 32CA reaction was characterized by an *ortho* regioselectivity and an *endo* stereoselectivity, in accordance with the experimental observation.
VI. The analysis of the solvent effects indicated that dichloromethane did not have any influence on the selectivity but it increased the activation energies and decreased the relative energies of the cycloadducts associated with this 32CA reaction.
VII. A thermodynamic parameters analysis showed that this 32CA was *ortho* regioselective and *endo* stereoselective, was under kinetic control and had exothermic and exergonic characters.

Author Contributions: Conceptualization, methodology, validation and review the article by A.K.N. Calculations, data curation, writing article draft by F.C. All authors have read and agreed to the published version of the manuscript.

Funding: This research received no external funding.

Institutional Review Board Statement: Not applicable.

Informed Consent Statement: Not applicable.

Data Availability Statement: Data contain within this article.

Acknowledgments: Our thanks are addressed to the Ministry of Higher Education and Scientific Research of the Algerian Government for supporting this work through the PRFU project, Code: B00L01EN210120220001.

Conflicts of Interest: The authors declare no conflict of interest.

References

1. Duarte, C.D.; Barreiro, E.J.; Fraga, C.A. Privileged structures: A useful concept for the rational design of new lead drug candidates. *Mini-Rev. Med. Chem.* **2007**, *7*, 1108–1119. [CrossRef] [PubMed]
2. Akhtar, J.; Khan, A.A.; Ali, Z.; Haider, R.; Yar, M.S. Structure-activity relationship (SAR) study and design strategies of nitrogen-containing heterocyclic moieties for their anticancer activities. *Eur. J. Med. Chem.* **2017**, *125*, 143–189. [CrossRef] [PubMed]
3. Liu, Y.; Hu, H.; Zhou, J.; Wang, W.; He, Y.; Wang, C. Application of primary halogenated hydrocarbons for the synthesis of 3-aryl and 3-alkyl indolizines. *Org. Biomol. Chem.* **2017**, *15*, 5016–5024. [CrossRef] [PubMed]
4. Zagórska, A.; Kołaczkowski, M.; Bucki, A.; Siwek, A.; Kazek, G.; Satała, G.; Bojarski, A.J.; Partyka, A.; Wesołowska. A Pawłowski, M. Structure–activity relationships and molecular studies of novel arylpiperazinylalkyl purine-2,4-diones and purine-2,4,8-triones with antidepressant and anxiolytic-like activity. *Eur. J. Med. Chem.* **2015**, *97*, 142–154. [CrossRef] [PubMed]
5. Kouadri, Y.; Ouahrani, M.R.; Missaoui, B.E.; Chebrouk, F.; Gherraf, N. Reactivity of b-Cetoesters Compounds, Synthesis of Nitrogenated Heterocycles (Derivatives of Tetrahydroacridin-9-ones and Pyrimidinone) and Biological Properties of Pyrimidinone Derivatives. *Asian J. Chem.* **2015**, *27*, 3675–3680. [CrossRef]
6. Xie, M.; Lapidus, R.G.; Sadowska, M.; Edelman, M.J.; Hosmane, R.S. Synthesis, anticancer activity, and SAR analyses of compounds containing the 5: 7-fused 4, 6, 8-triaminoimidazo [4,5-e][1,3] diazepine ring system. *Bioorg. Med. Chem.* **2016**, *24*, 2595–2602. [CrossRef]
7. Gomtsyan, A. Heterocycles in drugs and drug discovery. *Chem. Heterocycl. Comp.* **2012**, *48*, 7–10. [CrossRef]
8. Patterson, J.W.; Cheung, P.S.; Ernest, M.J. 3-Carboxy-5-methyl-N-[4-(trifluoromethyl) phenyl]-4-isoxazolecarboxamide, new prodrug for the antiarthritic agent 2-cyano-3-hydroxy-N-[4-(trifluoromethyl) phenyl]-2-butenamide. *J. Med. Chem.* **1992**, *35*, 507–510. [CrossRef] [PubMed]
9. Wagner, E.; Becan, L.; Nowakowska, E. Synthesis and pharmacological assessment of derivatives of isoxazolo [4 5-d] pyrimidine. *Bioorg. Med. Chem.* **2004**, *12*, 265–272. [CrossRef]
10. Huisgen, R. *1,3-Dipolar Cycloaddition Chemistry*; Wiley: New York, NY, USA, 1984; Volume 1, pp. 42–47.
11. Huisgen, R. 1, 3-dipolar cycloadditions. Past and future. *Angew. Chem.* **1963**, *2*, 565–598. [CrossRef]
12. Rios, R. Enantioselective methodologies for the synthesis of spiro compounds. *Chem. Soc. Rev.* **2012**, *41*, 1060–1074. [CrossRef] [PubMed]
13. Sun, J.; Xie, Y.J.; Yan, C.G. Construction of dispirocyclopentanebisoxindoles via self-domino Michael-aldol reactions of 3-phenacylideneoxindoles. *J. Org. Chem.* **2013**, *78*, 8354–8365. [CrossRef] [PubMed]
14. Shi, F.; Xing, G.J.; Zhu, R.Y.; Tan, W.; Tu, S. A catalytic asymmetric isatin-involved povarov reaction: Diastereo-and enantioselective construction of spiro [indolin-3, 2′-quinoline] scaffold. *Org. Lett.* **2013**, *15*, 128–131. [CrossRef] [PubMed]
15. Pal, S.; Khan, M.N.; Karamthulla, S.; Abbas, S.J.; Choudhury, L.H. One pot four-component reaction for the efficient synthesis of spiro [indoline-3,4′-pyrano [2,3-c] pyrazole]-3′-carboxylate derivatives. *Tetrahedron Lett.* **2013**, *54*, 5434–5440. [CrossRef]
16. Rapposelli, S.; Breschi, M.C.; Calderone, V.; Digiacomo, M.; Martelli, A.; Testai, L.; Vanni, M.; Balsamo, A. Synthesis and biological evaluation of 5-membered spiro heterocycle-benzopyran derivatives against myocardial ischemia. *Eur. J. Med. Chem.* **2011**, *46*, 966–973. [CrossRef]
17. Sadeghian, Z.; Bayat, M.; Safari, F. Synthesis and antitumor activity screening of spiro tryptanthrin-based heterocyclic compounds. *Med. Chem. Res.* **2022**, *31*, 497–506. [CrossRef]
18. Cheng, G.J.; Zhang, X.; Chung, L.W.; Xu, L.; Wu, Y.D. Computational organic chemistry: Bridging theory and experiment in establishing the mechanisms of chemical reactions. *J. Am. Chem. Soc.* **2015**, *137*, 1706–1725. [CrossRef]
19. Ríos-Gutiérrez, M.; Domingo, L.R. Unravelling the mysteries of the [3+2] cycloaddition reactions. *Eur. J. Org. Chem.* **2019**, *2–3*, 267–282. [CrossRef]
20. Jørgensen, K.A. *Cycloaddition Reactions in Organic Synthesis*; Wiley: New York, NY, USA, 2001.
21. Chafaa, F.; Hellel, D.; Nacereddine, A.K.; Djerourou, A. A theoretical study of the regio-and stereoselectivities of non-polar 1, 3-dipolar cycloaddition reaction between C-diethoxyphosphoryl-N-methylnitrone and N-(2-fluorophenyl) acrylamide. *Mol. Phys.* **2016**, *114*, 663–670. [CrossRef]
22. Chafaa, F.; Khorief Nacereddine, A.; Djerourou, A. Unravelling the mechanism and the origin of the selectivity of the [3+2] cycloaddition reaction between electrophilic nitrone and nucleophilic alkene. *Theor. Chem. Acc.* **2019**, *138*, 1–11. [CrossRef]
23. Nacereddine, A.K.; Layeb, H.; Chafaa, F.; Yahia, W.; Djerourou, A.; Domingo, L.R. A DFT study of the role of the Lewis acid catalysts in the [3+2] cycloaddition reaction of the electrophilic nitrone isomer of methyl glyoxylate oxime with nucleophilic cyclopentene. *RSC Adv.* **2015**, *5*, 64098–64105. [CrossRef]
24. Domingo, L.R.; Ríos-Gutiérrez, M.; Pérez, P. A molecular electron density theory study of the reactivity and selectivities in [3+ 2] cycloaddition reactions of C, N-dialkyl nitrones with ethylene derivatives. *J. Org. Chem.* **2018**, *83*, 2182–2197. [CrossRef]
25. Nacereddine, A.K.; Yahia, W.; Bouacha, S.; Djerourou, A. A theoretical investigation of the regio-and stereoselectivities of the 1, 3-dipolar cycloaddition of C-diethoxyphosphoryl-N-methylnitrone with substituted alkenes. *Tetrahedron Lett.* **2010**, *51*, 2617–2621. [CrossRef]
26. Teterina, P.S.; Efremova, M.M.; Sirotkina, E.V.; Novikov, A.S.; Khoroshilova, O.V.; Molchanov, A.P. A highly efficient and stereoselective cycloaddition of nitrones to N-arylitaconimides. *Tetrahedron Lett.* **2019**, *60*, 151063. [CrossRef]

27. Yahia, W.; Khorief Nacereddine, A.; Liacha, M.; Djerourou, A. A quantum-chemical DFT study of the mechanism and regioselectivity of the 1, 3-dipolar cycloaddition reaction of nitrile oxide with electron-rich ethylenes. *Int. J. Quantum Chem.* **2018**, *118*, e25540. [CrossRef]
28. Khorief Nacereddine, A.; Merzoud, L.; Morell, C.; Chermette, H. A computational investigation of the selectivity and mechanism of the Lewis acid catalyzed oxa-Diels–Alder cycloaddition of substituted diene with benzaldehyde. *J. Comput. Chem.* **2021**, *42*, 1296–1311. [CrossRef]
29. Lamri, S.; Heddam, A.; Kara, M.; Yahia, W.; Khorief Nacereddine, A. The Role of the Catalyst on the Reactivity and Mechanism in the Diels–Alder Cycloaddition Step of the Povarov Reaction for the Synthesis of a Biological Active Quinoline Derivative: Experimental and Theoretical Investigations. *Organics* **2021**, *2*, 57–71. [CrossRef]
30. Khorief Nacereddine, A. A MEDT computational study of the mechanism, reactivity and selectivity of non-polar [3+2] cycloaddition between quinazoline-3-oxide and methyl 3-methoxyacrylate. *J. Mol. Model.* **2020**, *6*, 1–12. [CrossRef]
31. Barama, L.; Bayoud, B.; Chafaa, F.; Khorief Nacereddine, A.; Djerourou, A. A mechanistic MEDT study of the competitive catalysed [4+2] and [2+2] cycloaddition reactions between 1-methyl-1-phenylallene and methyl acrylate: The role of Lewis acid on the mechanism and selectivity. *Struct. Chem.* **2018**, *29*, 1709–1721. [CrossRef]
32. Domingo, L.R. Molecular electron density theory: A modern view of reactivity in organic chemistry. *Molecules.* **2016**, *21*, 1319. [CrossRef]
33. Frisch, M.J.; Trucks, G.W.; Schlegel, H.B.; Scuseria, G.E.; Robb, M.A.; Cheeseman, J.R.; Scalmani, G.; Barone, V.; Mennucci, B.; Petersson, G.A.; et al. *Gaussian 09, Revision A.02*; Gaussian: Wallingford, CT, USA, 2009.
34. Lee, C.; Yang, W.; Parr, R.G. Development of the Colle-Salvetti correlation-energy formula into a functional of the electron density. *Phys. Rev.* **1988**, *37*, 785. [CrossRef]
35. Becke, A.D. Density-functional thermochemistry. I. The effect of the exchange-only gradient correction. *J. Chem. Phys.* **1992**, *96*, 2155–2160. [CrossRef]
36. Tomasi, J.; Persico, M. Molecular interactions in solution: An overview of methods based on continuous distributions of the solvent. *Chem. Rev.* **1994**, *94*, 2027–2094. [CrossRef]
37. Fukui, K. The path of chemical reactions-the IRC approach. *Acc. Chem. Res.* **1981**, *14*, 363–368. [CrossRef]
38. Simkin, B.I.; Sheĭkhet, I.I. *Quantum Chemical and Statistical Theory of Solutions—Computational Approach*; Ellis Horwood: London, UK, 1995.
39. Cances, E.; Mennucci, B.; Tomasi, J. A new integral equation formalism for the polarizable continuum model: Theoretical background and applications to isotropic and anisotropic dielectrics. *J. Chem. Phys.* **1997**, *107*, 3032–3041. [CrossRef]
40. Cossi, M.; Barone, V.; Cammi, R.; Tomasi, J. Ab initio study of solvated molecules: A new implementation of the polarizable continuum model. *Chem. Phys. Lett.* **1996**, *255*, 327–335. [CrossRef]
41. Barone, V.; Cossi, M.; Tomasi, J. Geometry optimization of molecular structures in solution by the polarizable continuum model. *J. Comput. Chem.* **1998**, *19*, 404–417. [CrossRef]
42. Becke, A.D. Density-functional thermochemistry. III. The role of exact exchange. *J. Chem. Phys.* **1993**, *98*, 5648. [CrossRef]
43. Parr, R.G.; Szentpály, L.V.; Liu, S. Electrophilicity index. *J. Am. Chem. Soc.* **1999**, *121*, 1922–1924. [CrossRef]
44. Parr, R.G.; Pearson, R.G. Absolute hardness: Companion parameter to absolute electronegativity. *J. Am. Chem. Soc.* **1983**, *105*, 7512–7516. [CrossRef]
45. Domingo, L.R.; Chamorro, E.; Pérez, P. Understanding the reactivity of captodative ethylenes in polar cycloaddition reactions. A theoretical study. *J. Org. Chem.* **2008**, *73*, 4615–4624. [CrossRef] [PubMed]
46. Domingo, L.R.; Pérez, P.; Sáez, J.A. Understanding the local reactivity in polar organic reactions through electrophilic and nucleophilic Parr functions. *RSC Adv.* **2013**, *3*, 1486–1494. [CrossRef]
47. Morell, C.; Grand, A.; Toro-Labbé, A. New dual descriptor for chemical reactivity. *J. Phys. Chem. A* **2005**, *109*, 205–212. [CrossRef]
48. Wiberg, K.B. Application of the pople-santry-segal CNDO method to the cyclopropylcarbinyl and cyclobutyl cation and to bicyclobutane. *Tetrahedron* **1968**, *24*, 1083–1096. [CrossRef]
49. Domingo, L.R. A new C–C bond formation model based on the quantum chemical topology of electron density. *RSC Adv.* **2014**, *4*, 32415–32428. [CrossRef]
50. Reed, A.E.; Weinstock, R.B.; Weinhold, F. Natural population analysis. *J. Chem. Phys.* **1985**, *83*, 735–746. [CrossRef]
51. Hellel, D.; Chafaa, F.; Nacereddine, A.K.; Djerourou, A.; Vrancken, E. Regio-and stereoselective synthesis of novel isoxazolidine heterocycles by 1, 3-dipolar cycloaddition between C-phenyl-N-methylnitrone and substituted alkenes. Experimental and DFT investigation of selectivity and mechanism. *RSC Adv.* **2017**, *7*, 30128–30141. [CrossRef]
52. Yahia, W.; Nacereddine, A.K.; Liacha, M. Towards understanding the role of Lewis acid on the regioselectivity and mechanism for the acetylation reaction of 2-benzoxazolinone with acetyl chloride: A DFT study. *Prog. React. Kinet. Mech.* **2014**, *39*, 365–374. [CrossRef]
53. Bayoud, B.; Barama, L.; Nacereddine, A.K.; Djerourou, A. Shedding light on the factors controlling the mechanism, selectivity and reactivity of the Diels–Alder reactions between substituted pyridinones and ethylenes: A MEDT study. *Mol. Phys.* **2021**, *119*, e1828635. [CrossRef]
54. Sobhi, C.; Nacereddine, A.K.; Nasri, L.; Lechtar, Z.; Djerourou, A. A DFT study of the mechanism and the regioselectivity of [3+ 2] cycloaddition reactions of nitrile oxides with α, β-acetylenic aldehyde. *Mol. Phys.* **2016**, *114*, 3193–3200. [CrossRef]

55. Geerlings, P.; De Proft, F.; Langenaeker, W. Conceptual density functional theory. *Chem. Rev.* **2003**, *103*, 1793–1874. [CrossRef] [PubMed]
56. Sobhi, C.; Nacereddine, A.K.; Djerourou, A.; Aurell, M.J.; Domingo, L.R. The role of the trifluoromethyl group in reactivity and selectivity in polar cycloaddition reactions. A DFT study. *Tetrahedron* **2012**, *68*, 8457–8462. [CrossRef]
57. Domingo, L.R.; Ríos-Gutiérrez, M.; Pérez, P. How does the global electron density transfer diminish activation energies in polar cycloaddition reactions? A Molecular Electron Density Theory study. *Tetrahedron* **2017**, *73*, 1718–1724. [CrossRef]
58. Sadi, S.; Khorief Nacereddine, A.; Djerourou, A. The effects of solvent nature and steric hindrance on the reactivity, mechanism and selectivity of the cationic imino-Diels–Alder cycloaddition reaction between cationic 2-azadienes and arylpropene. *J. Phys. Org. Chem.* **2022**, *35*, e4311. [CrossRef]
59. Domingo, L.R.; Sáez, J.A. Understanding the mechanism of polar Diels–Alder reactions. *Org. Biomol. Chem.* **2009**, *7*, 3576–3583. [CrossRef]
60. Domingo, L.R.; Aurell, M.J.; Pérez, P. A DFT analysis of the participation of zwitterionic TACs in polar [3+2] cycloaddition reactions. *Tetrahedron* **2014**, *70*, 4519–4525. [CrossRef]
61. Benchouk, W.; Mekelleche, S.M.; Silvi, B.; Aurell, M.J.; Domingo, L.R. Understanding the kinetic solvent effects on the 1, 3-dipolar cycloaddition of benzonitrile N-oxide: A DFT study. *J. Phys. Org. Chem.* **2011**, *24*, 611–618. [CrossRef]